ELSEVIER

Journal of Archaeological Science 35 (2008) 1125–1133

Journal of Archaeological SCIENCE

http://www.elsevier.com/locate/jas

Texture of *nopal* treated *adobe*: restoring Nuestra Señora del Pilar mission

Fernanda Martínez-Camacho [a], Javier Vazquez-Negrete [a], Enrique Lima [b,*], Victor Hugo Lara [b], Pedro Bosch [c]

[a] *Escuela Nacional de Conservación, Restauración y Museografía ''Manuel del Castillo Negrete'', INAH, Churubusco, México D.F., Mexico*
[b] *Departamento de Química, Universidad Autónoma Metropolitana, Iztapalapa, Av. San Rafael Atlixco No. 186, Col. Vicentina, 09340 México D.F., Mexico*
[c] *Instituto de Investigaciones en Materiales, Universidad Nacional Autónoma de México, Circuito Exterior, Ciudad Universitaria, 04510 México D.F., Mexico*

Received 23 July 2007; received in revised form 26 October 2007; accepted 26 October 2007

Abstract

Materials eroded, non-eroded, and treated with the local *nopal* mucilage *adobe*, from the Nuestra Señora del Pilar mission located in Sonora Mexico, are compared. The treatment of *adobe* bricks with an alcohol–water solution prior to the *nopal* application is proposed in order to increase their resistance to erosion. Using X-ray diffraction, small angle X-ray scattering, scanning electron microscopy and nitrogen adsorption techniques, we compared the structural and textural properties of eroded and non-eroded *adobe* materials. In the samples treated with *nopal* it is shown how the *nopal* coats the *adobe* small particles. The *nopal* impregnated material is stable up to 200 °C. A non-conventional distinction among these materials is made through fractal geometry and nitrogen adsorption. We also show through XRD measurements that erosion is homogeneous and not selective.

Keywords: *Adobe*; *Nopal*; Mucilage; Clay; Conservation; Colonial mission; Erosion; Fractal dimension; Diffusion; Adsorption

1. Introduction

Earth has been the most essential of building materials since the dawn of man. It is still often used even in modern architecture because it integrates to landscape, it is cheap and it offers convenient thermal properties. In this kind of architecture the earth building mixture is not kiln fired. At least 20 different traditions of earth construction are known, among which two major processes predominate: *pisé de terre* and *adobe* (Bardou and Arzoumanian, 1979; Guerrero and Fernando, 1994). The *pisé de terre* is applied to walls at least 50 cm thick by ramming earth between parallel frames that are removed revealing a completed section of hard earth wall. Although there is not a concept totally agreed for *adobe*; the term is applied to earth bricks shaped in moulds, sun dried and then used to build walls, vaults and domes. Traditionally, *adobe* bricks were never kiln fired. Adobe bricks are usually made with tightly compacted earth, clay and straw. However, construction methods and the composition of the *adobe* will vary according to climate and local customs.

Afterwards a layer of *adobe* plaster may be applied consisting of clay, sand, water, *nopal* juice (prickly pear cactus), horse manure and finely chopped wheat straw. This complex mixture creates a smooth coat as horse manure adds malleability and *nopal* is highly glutinous and adherent. The role of *nopal* is twofold: as a plasticizer for wet *adobe* plaster and as a superficial water repellent coating. Still, the type of *adobe* and plaster composition depends on the geographical zone as well as on the historical epoch.

In Mexico, *nopal* and corn straw have traditionally been used since Aztec times. Pre-Columbian temples and palaces

* Corresponding author. Tel.: +52 55 804 4667; fax: +52 55 804 4666.
E-mail address: lima@xanum.uam.mx (E. Lima).

0305-4403/$ - see front matter © 2007 Elsevier Ltd. All rights reserved.
doi:10.1016/j.jas.2007.10.019

present a facing which not only protected the earth from rain, but allowed geometrical and figurative motifs to be made of stones, baked bricks or polished ceramic, embedded in the walls during the construction. The Spanish colonial architecture of *adobe* construction is still clearly evident in most towns and cities all over America where many old missions, churches and buildings are still standing (Bainbridge, 1976).

As earth is an easily crumbling material, the degradation of earth architecture begins since the construction. Weather conditions such as wind, temperature (−4 to 40 °C), rain (Sonora rainfall since 1 October 2006 has been 1.08 m), or insect and bird nests are the main causes of deterioration. To these destruction mechanisms the human factor and the frequent earthquakes have to be added.

For the preservation and maintenance of architectural remains several solutions have been proposed based on the application of cement, polymer or sol-gel silica layers (Carretti et al., 2004; Erhardt, 2004; Tadanaga et al., 2000). Cement and polymeric materials present a relative lack of porosity and permeability; their application, then, is not compatible with *adobe*. Furthermore, if cement is added, compounds with different thermal properties are formed and they may separate with time and erosion. The same happens with polymers as they do not diffuse into the walls, and cracks may develop. The sol-gel technique is a very expensive method which has remained at laboratory level although it is rather promising (Dorge, 2000; Matsumoto et al., 2000).

The *adobe* missions in North Mexico and USA are often mentioned as a classical case of *adobe* fast deterioration. The previously mentioned restoration methods have not been effective; furthermore, some of them have accelerated the disintegration of bricks. A typical case is the Nuestra Señora del Pilar y Santiago de Cocóspera in Sonora, Mexico (Fig. 1). However, recently the traditional technique consisting of surface application of mucilage has seemed to provide better results. Mucilage is a high molecular weight pectic polysaccharide compound that occurs in *opuntia* cladodes and fruits.

Fig. 1. The Nuestra Señora del Pilar y Santiago de Cocóspera mission at Sonora, México.

Botanists recognize that *genus opuntia* is quite large. These plants, present in all Central and North Mexico, yield a wide range of soluble pectin (0.13 to 2.64 wt% on wet basis).

Still, the application of mucilage has provided results that are often questionable. Such controversy should be solved by understanding the mechanisms of consolidation, thus the distribution of mucilage into the building material. A standard procedure does not exist; in some cases the mucilage is sputtered straight forward, in others it is diluted and in some others the wall is pre-treated. A correlation between the application method and the depth of penetration has to be established. Indeed the role of mucilage, *i.e. nopal*, may be as consolidant or as water repellent. In this work the effect of a previous treatment of the wall on the mucilage distribution is studied. A water–alcohol treatment of the wall was chosen to reduce the surface tension of the *adobe* and promote the chemical interaction *adobe*–mucilage to ensure its consolidant action.

1.1. The Nuestra Señora del Pilar y Santiago de Cocóspera mission

The mission is located on a plateau in the middle of a valley in the Sonora desert. It is exposed to extreme temperatures, monsoon rains in summer and snow falls in winter. This mission was founded in ca. 1698 during the Spanish colonial period. The construction of this mission is attributed to Fray Eusebio Francisco Kino who decided to build it with *adobe* and to roof it with joists. The mission had to be repaired frequently as the Apaches and Seris attacked it continuously.

After the expulsion of Jesuits from the Spanish domains, the Franciscans occupied the mission; they rebuilt it following the contemporary taste, i.e. a baroque style with neoclassical influence. They refilled some walls with fired bricks, created altars, and modified the roof of the church, building a vault covered with a terrace. The vault collapsed at the end of the 19th century as a consequence of the abandonment of the church. No town was formed because of the constant attacks. The present building is a ruin (Fig. 1).

2. Experimental methods

2.1. Sampling

Eroded and non-eroded *adobe* materials from the Nuestra Señora del Pilar mission located in Sonora, Mexico were selected as follows. All samples were taken from the external wall of the church as the interior walls contain several superimposed materials which, through degradation processes, have favoured salt migration cycles. With a knife pieces of the wall were separated (around 500 mg). The depth was close to 0.5 cm. On the exterior of the building, garbage has been accumulated close to the walls at various heights. The freatic level and the evaporation surface of the wall are changing constantly. Thus, samples were taken at 150 cm from the garbage level from the South façade.

A reference sample was chosen from the building. It is a sample that was neither treated nor eroded. A second sample

was taken from an eroded zone of the wall. The third sample was selected from a wall treated with mucilage (*nopal*); this sample was taken after water evaporation. The last studied sample corresponds to a wall initially treated with a solution (50%) of water and alcohol (ethanol) and then treated with the mucilage. In all cases the mucilage application was by aspersion.

2.2. Characterization

2.2.1. X-ray diffraction

The samples were ground to be studied by X-ray diffraction (XRD) and small angle X-ray scattering (SAXS) techniques. Of course such treatment did not destroy the morphology present at a micron scale and they correspond to a surface 0.5 cm "thick". A Bruker-axs D8-advance diffractometer coupled to an X-ray diffraction copper anode tube was used to obtain the X-ray diffraction patterns which were recorded with a scintillation counter. A nickel filter selected the CuKα radiation. The identification of compounds was performed conventionally through the comparison with the JCPDS files.

2.2.2. Small angle X-ray scattering

Small angle X-ray scattering experiments were performed using a Kratky camera coupled to a copper anode X-ray tube whose Kα radiation was selected with a nickel filter. The collimated X-ray beam was linear and corresponded to an "infinitely high" beam geometry. The SAXS intensity data, $I(h)$, were collected with a linear proportional counter. Then they were processed with the ITP program (Glatter, 1981, 1988, 1991; Glatter and Hainisch, 1984) where the angular parameter, h in Å^{-1}, is defined as $h = 4\pi;\sin\theta/\lambda$, where θ and λ are the scattering angle and the X-ray wavelength, respectively. The powdered samples were introduced into a capillary tube. Measurement time was 9 min in order to obtain good quality statistics; indeed the linear proportional counter is like a multichannel system, therefore each point of the curve was measured for 9 min.

2.2.3. Scanning electron microscopy (SEM)

The morphology of the samples was established with a Leica Stereoscan 440 scanning electron microscope.

2.2.4. Nitrogen adsorption

Surface area analyses were performed on an Autosorb-1 Quantachrome apparatus. The N_2 adsorption–desorption isotherms were determined at -198 °C by volumetric adsorption. Before the N_2 adsorption process, all samples were outgassed at 80 °C for 12 h. Surface areas were calculated with the BET equation and pore diameter values with the BJH method.

2.2.5. Thermogravimetric analysis (TGA)

Thermogravimetric analyses were performed with TA Instruments equipment. Samples were treated at a heating rate of 5 °C min^{-1} from room temperature to 1000 °C in air.

3. Results and discussion

3.1. X-ray diffraction

As *adobes* are complex materials constituted by compounds with variable hardness the deterioration could be selective. Thus, the remaining wall material could be constituted by the stronger compounds. Fig. 2 compares the X-ray diffraction patterns of eroded and non-eroded *adobes*; they are similar, and they are both due to the following crystalline compounds: quartz, K-feldspars, plagioclase and a small amount of micaceous materials. Hence, erosion is homogeneous and not selective as occurs in other systems (Walderhaug, 1998). The following mechanism can be proposed based on the cementing effect of clays. If clays are selectively eroded, the *adobe* disaggregates homogeneously as there is no more agglomerating compound. The composition of the material still standing would be the same as the initial *adobe*. It could be suggested that erosion acts mainly at the grain boundary and produces a homogeneous crumbling of the surface by a progressive release of the grains as time goes on.

If the *adobe* is impregnated with the local mucilage (*nopal*), the diffractogram is not altered (Fig. 2). Therefore, the same compounds are present. Furthermore, no significant amount of amorphous material is added as the background line does not change. Thus, the amount of *nopal* incorporated into the samples, with or without a previous aspersion of the alcohol aqueous solution, is lower than 3% which is the minimum amount detected by X-ray diffraction.

3.2. Small angle X-ray scattering

SAXS is due to differences in the electron density. These differences have to be in the range 10 to 300 Å (diameter);

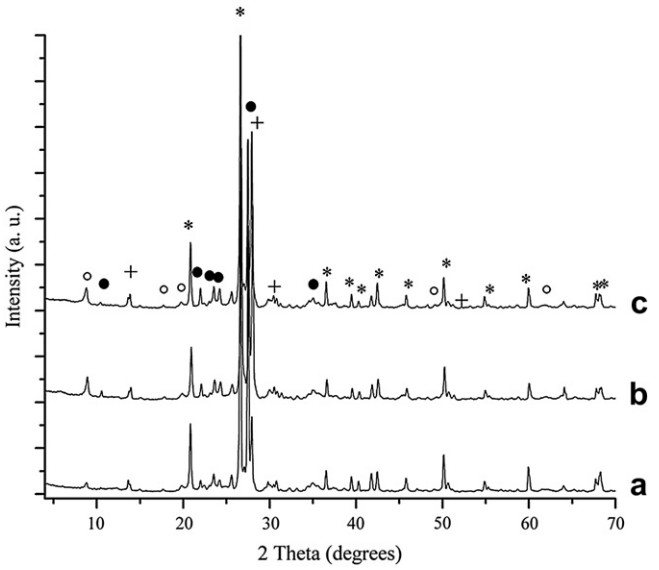

Fig. 2. XRD pattern of non-treated *adobe* (a); eroded *adobe* sample (b); *adobe* treated with alcohol–water and *nopal* (c). Compounds were indexed as quartz (*), muscovite (○), albite (+) and microcline (●).

they constitute heterogeneities which may be identified as pores or particles. The shape of those heterogeneities is estimated from the Kratky plot, i.e. $h^2I(h)$ vs. h. From this plot it is possible to assess whether the heterogeneities correspond to a fibrillar or a globular shape. If the Kratky curve presents a broad peak, the scattering heterogeneities most probably present a globular conformation whereas if the curve approximates a plateau the particles are fibril-like objects (Kataoka et al., 1993, 1994). If the shape is known, it is possible to calculate the distance distribution functions (Glatter, 1991; Glatter and Gruber, 1993). Finally, it is often useful to estimate, from the slope of the curve Log $I(h)$ against Log(h), the fractal dimension of the scattering objects (Harrison, 1995; Lima et al., 2004; Martin and Hund, 1987). For this study, the background obtained with the Porod plot was subtracted from the experimental intensity.

The dimension used in common life is Euclidean and corresponds to 3 for a volume (Cartesian system of three axes), 2 for a surface (Cartesian system of two axes) or 1 for a line. However surfaces may be corrugated and, therefore, cannot be described by a Cartesian two-axis system as it occupies a certain volume although it is not a thick and dense volume. The corresponding geometrical dimension is said to be between 2 and 3, thus it is a fractal dimension. A classic example may be dendritic growth (Guzmán et al., 2006; Harrison, 1995). Hence, if the *nopal* compound is retained partially through a strong interaction of an active section and the rest of it is loosely bound, the surface becomes more ''corrugated'' and the fractal dimension should be modified. Furthermore, the typical picture of abrupt electron density variations, in the shape of a battlement profile, due to the passage from particle to pore and *vice versa* turns out to be modified. Pore–particle–pore… frontiers are altered as *nopal* does not have the same electron density as the *adobe*. The frontier, then, is no longer abrupt; it is smooth, due to the progressive lowering of density. This effect can be characterized with the fractal dimension.

The Kratky curves of samples under study in this work are all representative of a fibrillar or slit-shaped scattering object. Assuming such shape, the particle size distribution (Fig. 3) of the non-treated *adobe* reveals that the radii of those fibrillar heterogeneities are 5 to 45 Å. It is not possible with this technique to identify the scattering heterogeneity. Furthermore, from the Babinet principle, it cannot be distinguished whether the heterogeneities are solid particles or pores. But, as in X-ray diffraction patterns, the peaks were narrow and they did not present any particle size effect; the particles are then larger than 300 Å (diameter) which implies that the SAXS observed heterogeneities are pores. Unfortunately, no difference between inter- and intra-particle porosity can be made if they are in the same size range. In this distribution, the main peaks are found for radii of 10, 25 and 40 Å (curve a); no significant contribution of pores with radii of 50 to 150 Å was observed.

In the eroded material (curve b) the proportion of large pores is larger than in non-treated *adobe*, as in the distribution the peak at 40 Å is enhanced. Again, no significant contribution of pores with radii of 50 to 150 Å was observed. Therefore, erosion could attack, first, the external layers of the

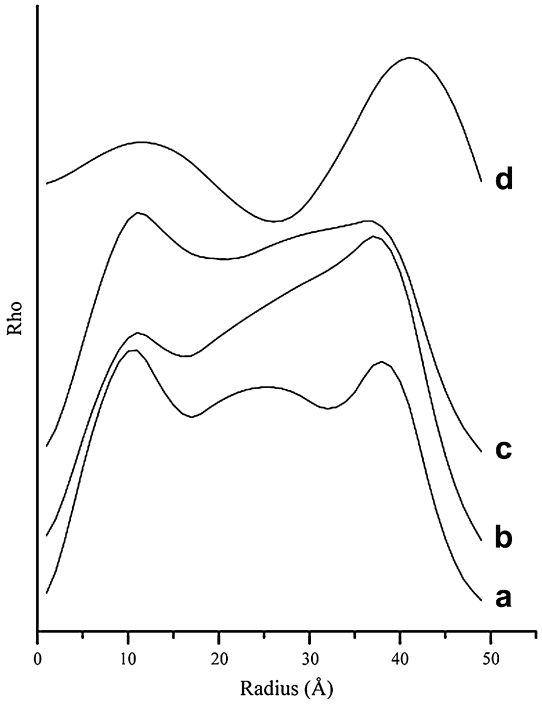

Fig. 3. Pore size distribution determined by SAXS of the non-treated *adobe* (a), eroded *adobe* sample (b), *nopal* treated *adobe* (c) and *adobe* treated with alcohol–water and *nopal* (d).

adobe, which are slightly burnished and, therefore, more compact. Another explanation could be that erosion excavates small pores, enlarging them.

When *nopal* is directly embedded, the pore size distribution (curve c) remains the same as the pore size distribution obtained for the initial *adobe*. Hence, either the amount of *nopal* retained is very small or the surface did not favour an interaction between the *nopal* and the porous network of the *adobe*.

The effect of alcohol before the impregnation with *nopal* is clearly shown by the size distribution (curve d). The mucilage occupies the small pores, mainly those whose radii are comprised between 15 and 30 Å. Then, a pore size distribution is generated whose pore radius is mainly 48 Å. In this sense, this material is texturally more homogeneous than the original *adobe* (curve a) or the *nopal* treated *adobe* (curve c).

The fractal dimension value (Fig. 4) was 2.3 for the alcohol spread sample impregnated with *nopal* and 2.8 for all other samples. As the fractal dimension is the same in the *nopal* embedded *adobe* as in the *adobe* itself the interaction between *nopal* and *adobe* must be very weak. Instead, as the value for the fractal dimension of the alcohol spread material impregnated with *nopal* is smaller than the value of the original material, the interaction of mucilage with the pore surface of *adobe* must be strong; the polymer is integrated to the porous network of the building material.

3.3. Scanning electron microscopy

The granular morphology of the well-preserved non-treated *adobe* is presented in Fig. 5. Most large agglomerates are

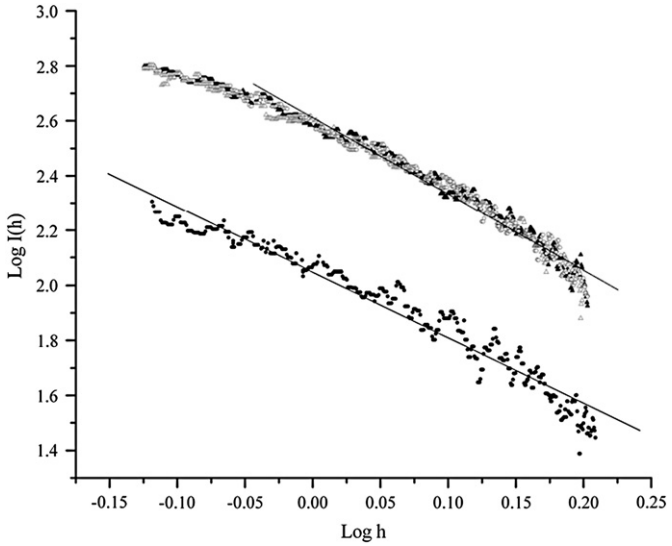

Fig. 4. Fractal dimension plots for the non-treated *adobe* (○); *adobe* after treating with *nopal* (▲); eroded *adobe* sample (△); *adobe* treated with alcohol–water and *nopal* (●).

constituted either by consolidated particles or by rather small particles stuck together. Some lamellar compounds were observed as the one located to the right of the central particle. They correspond to the feldspars reported in the X-ray diffraction study. The grain size is close to 100–140 μm.

With erosion, the grains (Fig. 6) turn out to be the same size and present a similar morphology. Hence the erosion alters only the nanometrical porous network although the general microscopic features (grain size, composition and morphology) remain. In a certain way, this observation favours the hypothesis that erosion enlarges small pores, bearing in mind that the range of sizes detected by SAXS is 10 to 300 Å (radii), and SEM images are in the micron domain. Particles or pores in the range 10 to 300 Å (radii) are beyond SEM resolution.

If the *adobe* is impregnated with *nopal*, again no significant modifications of the morphology are observed. Instead if the

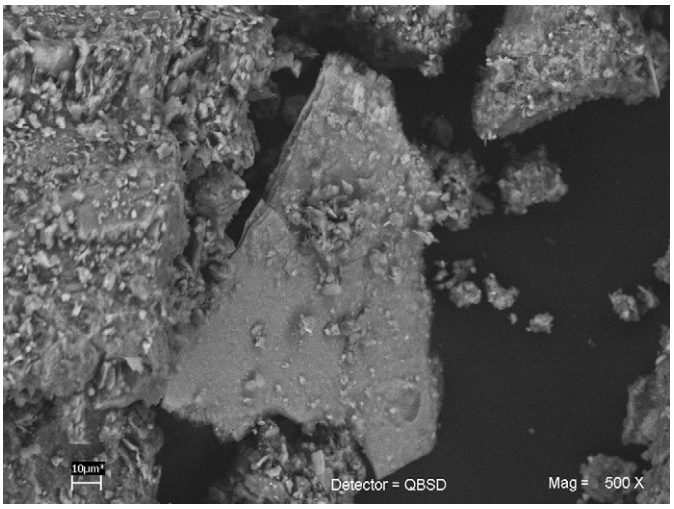

Fig. 5. Scanning electron microscopy image of a non-treated *adobe* sample from an interior wall (magnification: ×500).

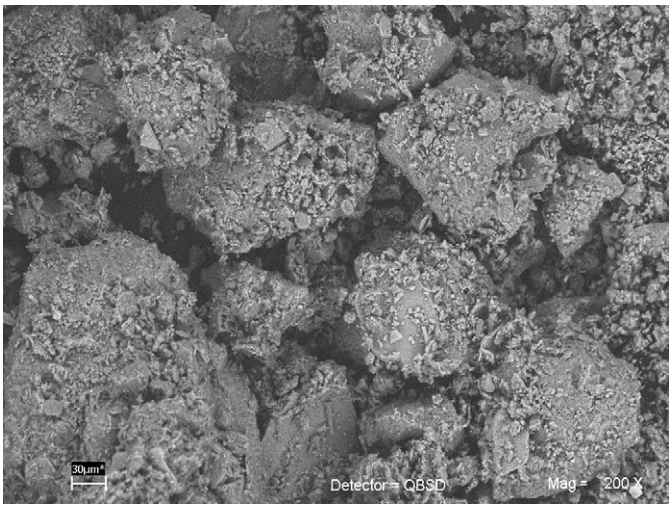

Fig. 6. Scanning electron microscopy image of an eroded *adobe* from an external wall (magnification: ×200).

nopal impregnation is preceded by an alcohol treatment, the texture of the obtained material presents more particles of ca. 2–8 μm which are more homogeneously distributed, revealing that the macroporous structure observed by SEM is due to the microporous size distribution determined by SA XS (Fig. 7). Note how the contrast varies if non-treated and alcohol–water and *nopal* samples are compared at a higher magnification, these differences may be attributed to *nopal* adhesion as determined by the other techniques. Our observations are only semi-quantitative as SEM is a local analysis technique and, thus, the statistical representation may be discussed. Still, *nopal* may fill the intraparticle pores in the micron range and be adhered to the external grain surface.

3.4. N_2 isotherms

N_2 adsorption–desorption isotherms of the samples under study are displayed in Fig. 8. As the curves are convex to P/P_0 axis (no point B is observed) the isotherms are of the type II in the IUPAC classification, revealing a very weak adsorbate–adsorbent interaction. All the isotherms present a type III hysteresis loop, characteristic of platy particles or adsorbents containing slit-shaped pores. However, a difference is noted: the pre-treated *nopal* sample adsorbs a lower total volume. The adsorption isotherm remains at a very low level, even at high P/P_0 values, which suggests that the proportion of big mesopores decreases significantly after filling by *nopal.*

The specific surface areas (SA), as determined by the Brunauer–Emmet–Teller equation, are reported in Table 1. They are very low due to the small amount of weakly adsorbed N_2. As the SA values of the untreated *adobe* and the eroded *adobe* sample are the same, not only the composition but also the texture of *adobe* remains unaltered as shown by XRD. The pore size distribution obtained by SAXS is in disagreement with such a conclusion. However, it has to be emphasized that SAXS is sensitive to closed pores or ink bottle-shaped pores

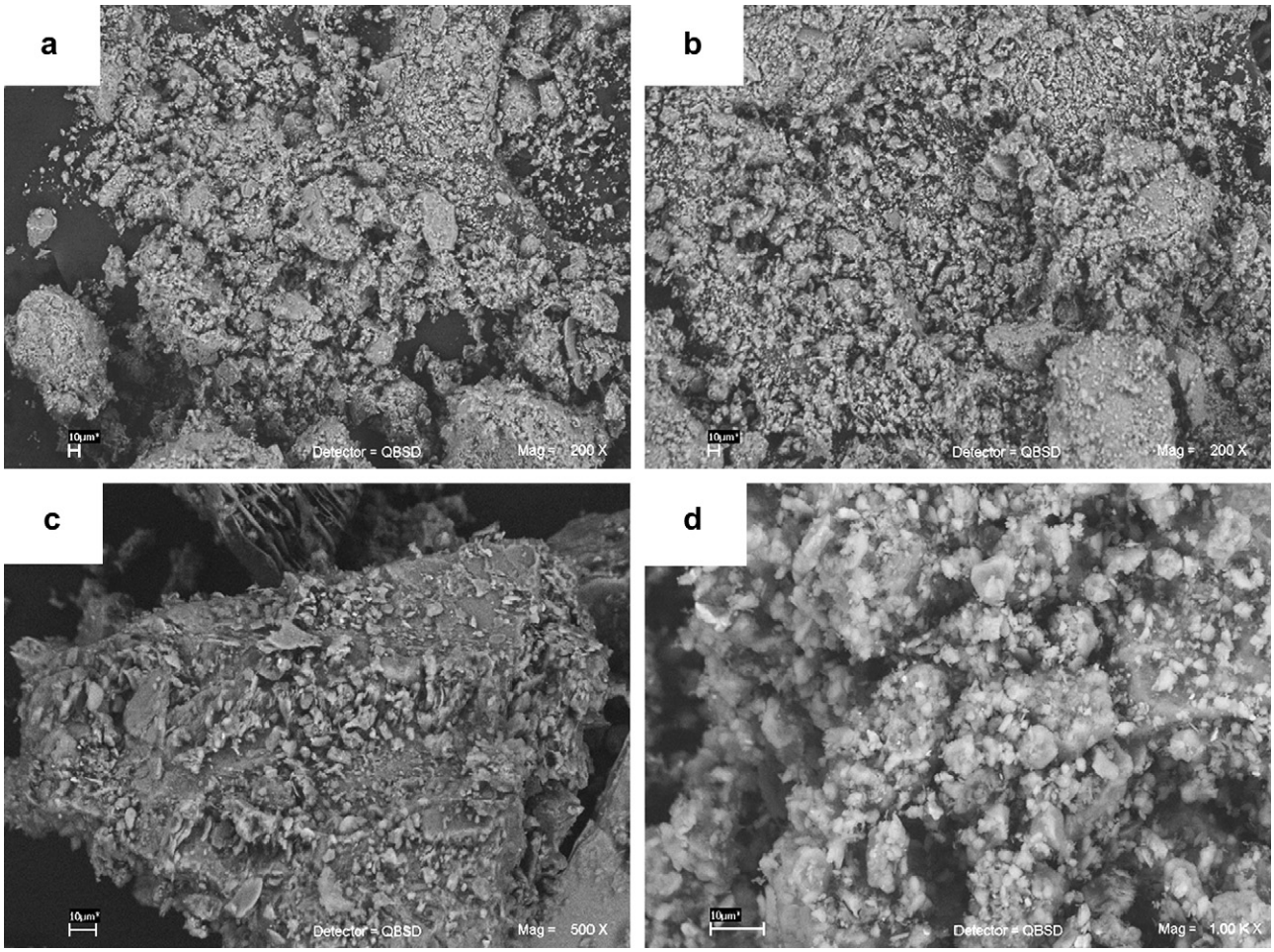

Fig. 7. Scanning electron microscopy image of the *nopal* treated *adobe* (a); the *nopal* treated *adobe* with the alcohol–water application (b) and (d); untreated *adobe* (non-eroded) (c).

which cannot be reached by nitrogen molecules. Thus, erosion acts by excavating small pores and shaping them as ink bottle.

When the non-treated *adobe* and the sample embedded with *nopal* are compared, the corresponding SA values are similar revealing that *nopal* does not fully impregnate *adobe* particles and does not reach the core, the adsorption is external. Lastly, if the eroded sample and the sample treated with alcohol and then impregnated with *nopal* are compared, the difference in SA shows that *nopal* reduces the SA significantly, suggesting that mucilage wets partially the *adobe* or interacts strongly with the *adobe* pore network.

These observations agree with the pore size determined by the BJH method from the desorption step. The obtained values are 113, 136 and 169 Å (pore diameter) for the non-treated sample, the eroded sample, and the *nopal* impregnated sample, respectively. Again the trend of the values seems to indicate that the *nopal* partially fills the small pores and the resulting mean pore size is larger than in the original *adobe*. The differences between these mean values and the SAXS distributions have to be attributed to the principles of the techniques. Again, adsorption measurements correspond to nitrogen gas accessible to pores, whereas SAXS values correspond to open and closed pores (bubbles or ink bottle-shaped pores).

Instead, the pore diameter is 86 Å for the alcohol treated material and impregnated with *nopal*. This value is in very good agreement with the maximum of the size distribution determined by SAXS (radius of 48 Å).

3.5. Thermal analysis

To understand the weight loss curves (Fig. 9), the pure *nopal* curve was first obtained. Three steps are identified: 15% (wt) from room temperature to 230 °C, 40% from 230 to 350 °C, and 10% from 350 up to 700 °C.

The comparative study of the weight loss curves as a function of temperature shows that the non-treated sample loses 0.7% from room temperature up to 100 °C, which is attributed to water. The material becomes rather stable up to 400 °C as only 0.5% weight is lost in this large temperature interval. Lastly, it loses 2%, corresponding most probably to a dehydroxylation process. Instead, the two treated materials, after the water loss, from 230 to 350 °C, lose 0.5% more than the free *nopal* sample. This weight loss has to be assigned to *nopal* decomposition. Hence, the amount of retained mucilage is at least close to 0.5%. A second weight loss from 300 to 450 °C is observed; this step is not found either in the *adobe*

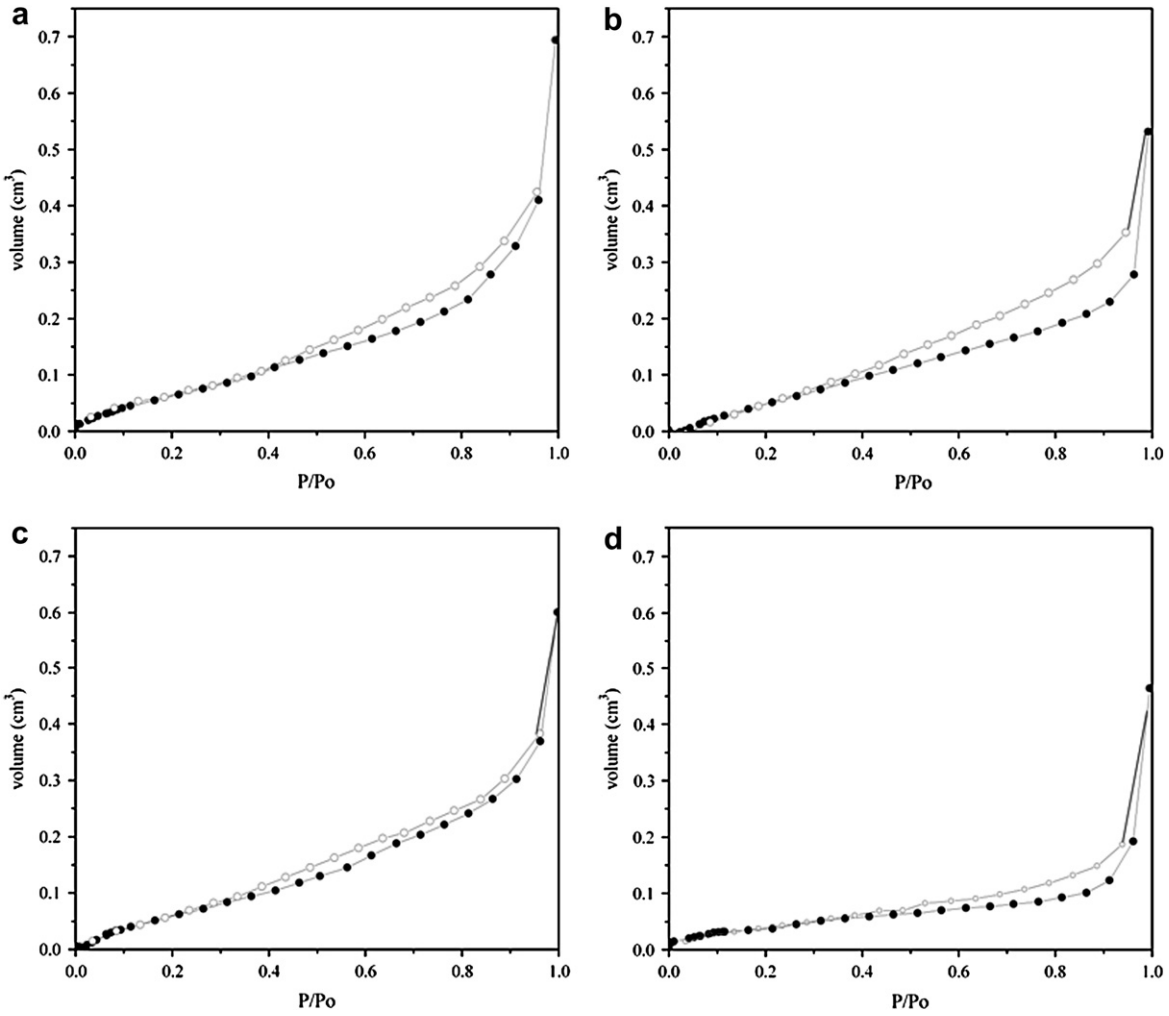

Fig. 8. N_2 adsorption (-●-) desorption (-○-) isotherms on samples: untreated *adobe* (reference sample) (a); *adobe* after treating with *nopal* (b); *adobe* (eroded sample) (c); *adobe* treated with alcohol–water and *nopal* (d).

or in the pure mucilage samples. Then, it has to correspond to a fraction (0.6%) of *nopal* strongly adsorbed on the *adobe* surface. Note that the curves of the *nopal* treated materials behave differently at high temperatures (450 to 700 °C). The *nopal* treated sample loses less weight and reproduces the shape of the *adobe* sample, hence, no more mucilage is present or, in other words, no mucilage is present that interacts strongly. The previously alcohol-treated sample and impregnated with *nopal* loses 0.2% more, which has to be understood as

Table 1
Specific surface area of the *adobe* samples, as determined from the N_2 adsorption–desorption isotherms and the BET equation and average pore size determined by the BJH method

Sample	Specific surface area, SSA, (m^2/g)	Pore diameter (Å)
Untreated *adobe*	13.67	113
Adobe treated with *nopal*	13.44	169
Eroded *adobe* sample	13.09	136
Adobe treated with alcohol–water and *nopal*	7.03	86

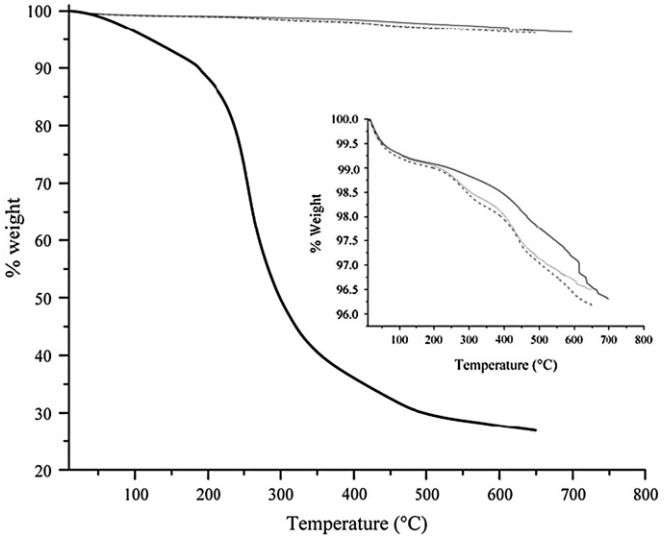

Fig. 9. Thermogravimetric curves of *nopal* (▬), non-treated *adobe* (–), *nopal* treated *adobe* (…) and *nopal* treated *adobe* with previous alcohol–water application (- - -). Inset: curves in the 100–95% weight loss window.

a dehydroxylation of the alcohol modified surface as mucilage does not decompose at such a temperature range.

We return now to explain the loss of ca. 6 m^2/g of SA following the treatment with alcohol–water and *nopal*, due to the occlusion of pores. In this case pores are assumed to be cylindrical with radius r, then the surface loss is 6.64 $m^2 = 2\pi(N)(r)(h)$, where r is the radius of the cylindrical pore, h is the height of the cylindrical pore and N is the number of occluded pores: the surface lost is the lateral surface of the cylinders.

Thermal analyses show that the amount of mucilage retained is close to 1%. Hence, 1 g of *adobe* retains 0.01 g of mucilage whose density is assumed to be close to 1. Thus, 0.01 cm^3 of polymer are retained. In terms of r and h, the cylindrical volume occluded is then: $0.01 = (N)(\pi)(r^2)(h)$. The radius of the cylindrical pores filled should be close to 25–30 Å. This result agrees with the SAXS values, pointing out that pores with radii sized in this interval decrease from non-treated *adobe* sample to *nopal* treated sample with a previous alcohol-treatment (Fig. 3a and d).

3.6. Adsorption mechanism

To summarize, *adobe* composition and texture is not altered by erosion as revealed by N_2 adsorption, scanning electron microscopy and X-ray diffraction. The corresponding pore morphology is maintained, as shown by small angle X-ray scattering but an ink bottle-shaped porosity appears with excavation of small pores. Therefore, with erosion there is no selective destruction of any of the crystalline compounds.

When *adobe* is impregnated with *nopal* the mucilage is retained. If a previous treatment with an alcohol solution is performed, a thin layer of organics covers the *adobe* particles and adheres to the pore walls, promoting then a more homogeneously distributed texture as shown by scanning electron microscopy, thermal analyses and small angle X-ray scattering.

On the one hand, the treatment with alcohol is expected to hydrolyse the surface, generating a hydroxyl enriched layer. On the other, the *nopal* solution is mainly constituted by mucilage which is a polymer whose composition includes galactose, arabinose and uronic acid (Goycoolea and Cárdenas, 2003). The polar functional groups (carbonyls, alcohols, amines among others), present in mucilage molecules, are prone to interact with the OH enriched surface through hydrogen bonds. They interact with the wall and filling pores ,and consolidate the *adobe* particles.

In previous and more conventional works (Cárdenas et al., 2004; Metcalfe, 1993), research has been focused on the effect of pH or molarity on the *nopal* solution and on the mucilage deposition. In this work, we have found that the treatment of the *adobe*, previous to *nopal* deposition, stabilizes the layer of organics as shown by our results. The parameter to be improved is not the gelling rate but the intergranular diffusion. A fast gelling rate would only promote an external deposition, which, with time, will fracture the material. Instead, a slow diffusion of the solution embeds the *adobe*, the *nopal* then gels in the inter-granular space; a homogeneous stronger material is then obtained whose surface area is much lower as shown by N_2 adsorption measurements. If the area is reduced the surface exposed to air and water is less, and the erosion should diminish. Still, if other weathering mechanisms occur, such as crystallization and freeze thawing, this effect can be reversed.

4. Conclusion

Eroded and non-eroded *adobe* materials from the Nuestra Señora del Pilar mission located in Sonora Mexico were compared. Quartz, K-feldspars, plagioclase and some micaceous material were the main crystalline compounds present in the *adobe*. No effect on the composition was observed in the weather eroded samples, thus the degradation is not selective and only small pores are excavated.

If the *adobe* was treated with the local *nopal* mucilage, it behaved in a very different way depending on the application procedure. Due to the reduction of surface tension, the addition of an alcohol–water solution prior to the *nopal* application appears to improve the mucilage diffusion in *adobe*. The mucilage coats the hydroxylated *adobe* small particles occupying the small pores. The thermal behaviour shows that the *nopal* impregnated material is stable up to 200 °C. A non-conventional distinction among these materials is made through fractal dimension. This parameter shows the interaction strength between mucilage and pore walls. With the alcohol treatment the mucilage is incorporated in the *adobe* texture and develops an irregular surface. Without treatment the interaction is very weak.

Acknowledgements

Thanks are due to Leticia Baños, Esteban Fregoso and José Guzmán for the technical work in XRD, TGA and SEM, respectively.

References

Bainbridge, B., 1976. Early Architecture in New Mexico. University of New Mexico Press, Albuquerque.

Bardou, P., Arzoumanian, V., 1979. Arquitecturas de *adobe*. Gustavo Gil Madrid.

Cárdenas, A., Argüelles, W.M., Goycoolea, F.M., 2004. Revista Iberoamericana de Polímeros 5, 46.

Carretti, E., Dei, L., Macherelli, A., Weiss, R.G., 2004. Rheoreversible polymeric organogels: the art of science for art conservation. Langmuir 20, 8414–8418.

Dorge, V., 2000. The Gels Cleaning Research Project. The Getty Conservation Institute Newsletter, vol. 15, 16–20.

Erhardt, D., 2004. The art of restoration. Nature 431, 410–411.

Glatter, O., 1981. Convolution square root of band-limited symmetrical functions and its application to small-angle scattering data. J. Appl. Cryst. 14, 101–108.

Glatter, O., 1988. Comparison of two different methods for direct structure analysis from small-angle scattering data. J. Appl. Cryst. 21, 886–890.

Glatter, O., 1991. Scattering studies on colloids of biological interest (amphiphilic systems). Prog. Colloid Polymer Sci. 84, 46–54.

Glatter, O., Gruber, K., 1993. Indirect transformation in reciprocal space: desmearing of small-angle scattering data from partially ordered systems. J. Appl. Cryst. 26, 512–518.

Glatter, O., Hainisch, B., 1984. Improvements in real-space deconvolution of small angle scattering data. J. Appl. Cryst. 17, 435–441.

Goycoolea, F.M., Cárdenas, A., 2003. Pectins from Opuntia spp.: a short review. J. PACD, 17–29.

Guerrero, B., Fernando, L., 1994. Arquitectura de tierra en México. UAM, Azcapotzalco, Mexico.

Guzmán, A., Lima, E., Delahay, G., Coq, B., Lara, V., 2006. Complementary physicochemical characterization by SAXS and 129Xe NMR spectroscopy of Fe-ZSM-5: influence of morphology in the selective catalytic reduction of NO. Ind. Eng. Chem. Res. 45, 4163–4168.

Harrison, A., 1995. Fractals in Chemistry. Oxford University Press, New York.

Kataoka, M., Hagihara, Y., Mihara, K., Goto, Y., 1993. Molten globule of cytochrome c studied by small angle X-ray scattering. J. Mol. Biol. 229, 591–596.

Kataoka, M., Flanagan, J.M., Tokunaga, F., Engelman, D.M., 1994. Use of X-ray solution scattering for protein folding study. In: Chance, B., et al. (Eds.), Synchrotron Radiation in the Biosciences. Clarendon Press, Oxford, UK, pp. 187–194.

Lima, E.J., Lara, V.H., Bulbulian, S., Bosch, P., 2004. Fractal dimension and cobalt leaching in CoX and CoA zeolites. Chem. Mater 16, 2255–2258.

Martin, J.E., Hund, A.J., 1987. Scattering from fractals. J. Appl. Cryst. 20, 61–78.

Matsumoto, T., Murakami, Y., Takasu, Y., 2000. Size control of titanium oxide sheets by regulating catalysis in a catalytic sol-gel process and their UV absorption properties. J. Phys. Chem. B 104, 1916–1920.

Metcalfe, J.L., 1993. Conservation at Mission San Xavier del Bac. WAAC Newslett 15, 20–23.

Tadanaga, K., Morinaga, J., Matsuda, R., Minami, T., 2000. Superhydrophobic-superhydrophilic micropatterning on flowerlike alumina coating film by the sol-gel method. Chem. Mater. 12, 590–592.

Walderhaug, O., 1998. Chemical weathering at rock art sites in Western Norway: which mechanisms are active and how can they be retarded? J. Archaeol. Sci. 25, 789–800.